ingegneria sismica
International Journal of Earthquake Engineering
Anno XLII – Num. 4 - 2025

Sequential seismic and settlement analysis of reinforced concrete moment-resisting frames

Mehmet Yigitbas, Ernesto Grande and Maura Imbimbo*

Department of Civil and Mechanical Engineering, University of Cassino and Southern Lazio, 03043, Cassino FR, Italy

SUMMARY: *Reinforced concrete (RC) moment-resisting frames located in liquefaction-prone areas may experience foundation settlements shortly after strong earthquakes, when the structure has already undergone inelastic deformation and residual damage. In current engineering practice, settlement effects are often evaluated assuming an undamaged structural configuration, potentially leading to unconservative post-earthquake assessments. This study investigates the influence of seismic-induced damage on the subsequent settlement response of RC frames through a decoupled sequential analysis framework that preserves the residual mechanical state attained at the end of the earthquake. Two-storey and four-storey, three-bay RC frames representative of modern Strong Column/Weak Beam and older Strong Beam/Weak Column design philosophies are analysed. Seismic damage is first introduced by nonlinear dynamic time-history analyses using spectrum-compatible ground motions. Foundation settlements are then imposed through nonlinear static analyses by prescribing vertical displacements at the supports via compression-only soil–structure interface elements. The results show that global settlement mechanisms, including axial force redistribution and alternative load paths, are primarily governed by structural geometry and settlement profile, and are only marginally affected by prior seismic damage. Conversely, the local response is strongly influenced by the residual seismic state: permanent curvatures and plastic deformations accumulated during the earthquake significantly reduce the available ductility during the settlement phase. The findings highlight the limitations of settlement assessments based on undamaged models and support the adoption of sequential analysis strategies for a reliable post-earthquake evaluation of RC frames.*

KEYWORDS: post-earthquake settlement, sequential analysis, reinforced concrete frames, seismic damage state, local ductility demand

1 Introduction

Structures located in seismically hazardous areas are always exposed to multiple hazard sequences that can occur after an earthquake. As revealed by damage assessment studies conducted in the short and long term after an earthquake, foundation settlements caused by soil liquefaction, cyclic softening, or loss of bearing capacity are among the most critical events following an earthquake. It is known that these settlements can occur shortly after the seismic event, especially when the structure is still damaged and mechanically vulnerable. Although

*mehmet.yigitbas@unicas.it
https://doi.org/10.65102/is202545
Published: 20 February, 2026

seismic design codes primarily address the transient effects of ground acceleration, these permanent vertical ground deformations can impact the structural performance and safety of buildings after an earthquake.

Traditional single hazard assessments create a vulnerability by failing to account for the interaction between seismic damage and settlement occurring immediately after an earthquake. RC frames enter a nonlinear range during strong seismic activity and are exposed to permanent effects such as loss of rigidity, cracking, plastic hinge formation, and permanent inter-story drifts. When foundation settlements, frequently observed in liquefiable soils, occur immediately after a ground shake, they affect a structure that has already partially lost its deformation capacity. Consequently, in this situation, the structural response to settlement is fundamentally different from that of an undamaged or elastic system.

Despite this physical evidence, current engineering practices generally treat seismic damage and settlement effects as independent events. Settlement demands are usually evaluated using undamaged structural models that implicitly assume elastic behaviour and full rigidity recovery after an earthquake. However, in a structure where significant inelastic deformation and permanent damage have occurred, these assumptions are no longer valid. Therefore, neglecting the effects of earthquakes, including permanent plastic rotations and loss of rigidity, can lead to post-earthquake assessments that are not conservative, resulting in underestimation of local failure and repairability issues.

Clearly, there is a need for analytical frameworks that can account for structural changes and permanent damage caused by earthquakes. It is vital to understand how permanent damage affects force redistribution mechanisms, local ductility demand and settlement capacity in order to define realistic performance limits and post-earthquake decision criteria for reinforced concrete buildings in liquefaction-prone areas.

The present study addresses this need by investigating the sequential effects of seismic damage and post-earthquake foundation settlements through a structural-focused numerical framework. A decoupled sequential analysis strategy is adopted to preserve the damaged mechanical state induced by earthquake loading and to evaluate its influence on the subsequent settlement response of RC moment-resisting frames designed according to different detailing philosophies.

2 State of the art and research gap

Existing research has extensively investigated the seismic response of reinforced concrete (RC) buildings and, separately, the effects of permanent ground deformations such as liquefaction-induced settlements and lateral spreading. Classical contributions by Burland and Wroth [1], Boscardin and Cording [2], and Skempton and MacDonald [3] established widely adopted criteria for damage classification and allowable differential settlements under static or construction-related conditions. While these studies provide a fundamental reference for serviceability and damage assessment, they implicitly assume an undamaged or elastic structural configuration and therefore do not address scenarios in which settlements act on structures that have already experienced significant inelastic deformation due to seismic loading.

Post-earthquake field observations and reconnaissance studies in liquefaction-prone regions have clearly shown that such sequential hazard scenarios are not exceptional. Several earthquake events have documented cases in which buildings first sustained severe inertial damage during shaking and subsequently experienced substantial differential settlements during or after soil reconsolidation [4, 5]. These observations highlight that seismic damage and settlement effects often develop in a chronological sequence and interact through the altered mechanical

state of the structure. Consequently, assessment procedures treating seismic damage and settlement demand as independent phenomena are inherently limited in their ability to represent post-earthquake structural performance.

From a numerical modelling perspective, one of the two main strategies developed to address the interaction between seismic loading and settlement is fully coupled soil-structure interaction (SSI) analysis. This modelling method has the significant advantage of simultaneously simulating ground motion, ground nonlinearity and liquefaction-induced deformations within a single dynamic framework, enabling the realistic capture of interaction effects [6, 7, 8]. Despite their comprehensive physical nature, advanced structural soil models require detailed calibration and significant computational effort, which presents serious feasibility problems and currently limits their applicability to research-oriented studies and highly case-specific analyses.

Conversely, uncoupled or sequential frameworks are free from these disadvantages. In these frameworks, the seismic response of structures is first evaluated and then settlement is applied to the damaged configuration. The modelling flexibility offered, the significant reduction in computational cost and compatibility with existing structural analysis tools make this alternative method important for parametric studies and engineering applications [9, 10, 11]. However, the reliability of this model depends on how accurately it can transfer residual damage, permanent deformation and stiffness degradation caused by seismic loading between series of analyses.

Several studies adopting sequential or uncoupled frameworks have demonstrated that residual seismic damage can significantly influence settlement response. Analyses on RC frames subjected to differential settlements have shown that sections remaining elastic under settlement-only conditions may yield or reach failure when the same settlement profiles are applied after seismic loading [9, 11, 12] . At the same time, other contributions have reported that global settlement mechanisms, such as axial force redistribution and overall stability, may remain largely unaffected by prior seismic damage [10, 13]. These findings suggest a potential decoupling between global equilibrium mechanisms and local failure processes under post-earthquake settlement conditions.

Despite advances in seismic research, there are still significant gaps in our understanding of how structures respond to settlement. Many existing studies focus on simplified structural configurations, specific settlement models or limited seismic intensity ranges. They generally do not compare undamaged and post-earthquake settlement responses systematically within a single analytical framework [9, 10, 11, 12, 13]. Furthermore, the distinction between global equilibrium mechanisms and local failures driven by curvature ductility demand is often unclear or not analysed quantitatively. Consequently, the effect of seismic-induced state changes on ductility reduction and increased local settlement demand remains unclear.

This study focuses on the effect of seismic-induced state changes on the settlement fragility of RC moment-resisting frames. A decomposed sequential analysis strategy is used to compare settlement and earthquake-settlement scenarios. It distinguishes between global response mechanisms and local damage evolution, highlighting the effects of residual seismic damage for post-earthquake assessment and engineering decision-making processes.

2.1 Objectives and scope of the study

The main objective of this study is to investigate the effect of earthquake-induced damage on the post-earthquake settlement response of reinforced concrete (RC) moment-resisting frames. The problem with traditional assessments is that they evaluate settlement effects by assuming that structures are undamaged and elastic. In contrast, our approach considers the permanent

mechanical state caused by previous seismic loading when evaluating the demand resulting from post-earthquake settlement.

To this end, we have adopted a decoupled sequential analysis framework to quantify the effects of seismic-induced stiffness degradation, residual deformations and local ductility consumption on the structural response to applied vertical ground displacements. Within the scope of this study, the approach that settlement affects a structure whose mechanical properties and deformation capacity vary due to seismic loading has been adopted.

By adopting two representative RC frame typologies, the role of structural design philosophy has been examined through comparative analysis:

(a) strong column/weak beam (SC/WB) frames, which represent modern seismic design practice based on capacity design principles.

(b) strong beam/weak column (SB/WC) frames, which represent older, non-ductile structures typical of designs prior to the 1970s.

This comparison evaluates the effect of different damage distributions resulting from seismic loading on local failure mechanisms and residual settlement capacity.

Furthermore, the sensitivity of structural response was examined by considering different settlement types, ranging from moderately differentiated settlements to high-gradient configurations. This parametric evaluation clarifies how the geometry of the applied ground deformation interacts with the resulting seismic damage state. By jointly analysing global response mechanisms and local damage accumulation, the study provides a rational basis for post-earthquake assessment of RC frames subjected to foundation settlements, with specific emphasis on ductility demand, repairability, and performance evaluation.

3 Case studies, modeling approach and numerical analyses

3.1 Case-study

The case studies considered in this paper consist of two planar RC moment-resisting frames, namely a two-storey three-bay and a four-storey three-bay configuration (Figure 1), selected to illustrate the proposed vulnerability analysis and to discuss the role of building height and vertical development on susceptibility to imposed ground deformations. The two frames share the same bay length and the same member cross-sections, so that the comparison is not biased by gross geometric differences and the observed variations in response can be primarily attributed to structural topology and reinforcement detailing.

To represent distinct design eras and detailing philosophies, two reinforcement layouts are considered for each geometry: (i) a Strong Column / Weak Beam (SC/WB) configuration, representative of modern capacity design concepts and ductile detailing (e.g., Eurocode 8 [14]), and (ii) a Strong Beam / Weak Column (SB/WC) configuration, representative of older, non-ductile construction practices. The intended change in design philosophy is achieved by modifying only the longitudinal reinforcement, while keeping the member sizes unchanged. Columns have a 300×300 mm cross-section and beams a 300×500 mm cross-section; the corresponding longitudinal reinforcement arrangements for columns and beams, as a function of the number of storeys and design philosophy, are reported in Figure 1.

Both frame typologies are assumed to be supported by a flexible foundation system representative of isolated footings, which allows differential vertical movements among column bases. Within this assumption, the structural response is investigated through a nonlinear sequential framework in which strong-motion excitation is first applied to induce a damaged resid-

ual state, and spatially variable vertical displacements are subsequently imposed to simulate post-earthquake settlement demand. In order to maintain a structural-oriented and computationally efficient modelling strategy, the analysis is not performed through fully coupled soil–structure interaction models, which are generally more demanding and less straightforward to generalize for parametric comparisons. Instead, settlements are imposed through controlled boundary displacements applied at dedicated soil nodes, connected to the column base nodes by means of zero-length interface elements with appropriate unilateral (compression-only) behaviour, thus allowing loss of contact and preventing spurious tensile reactions at the supports.

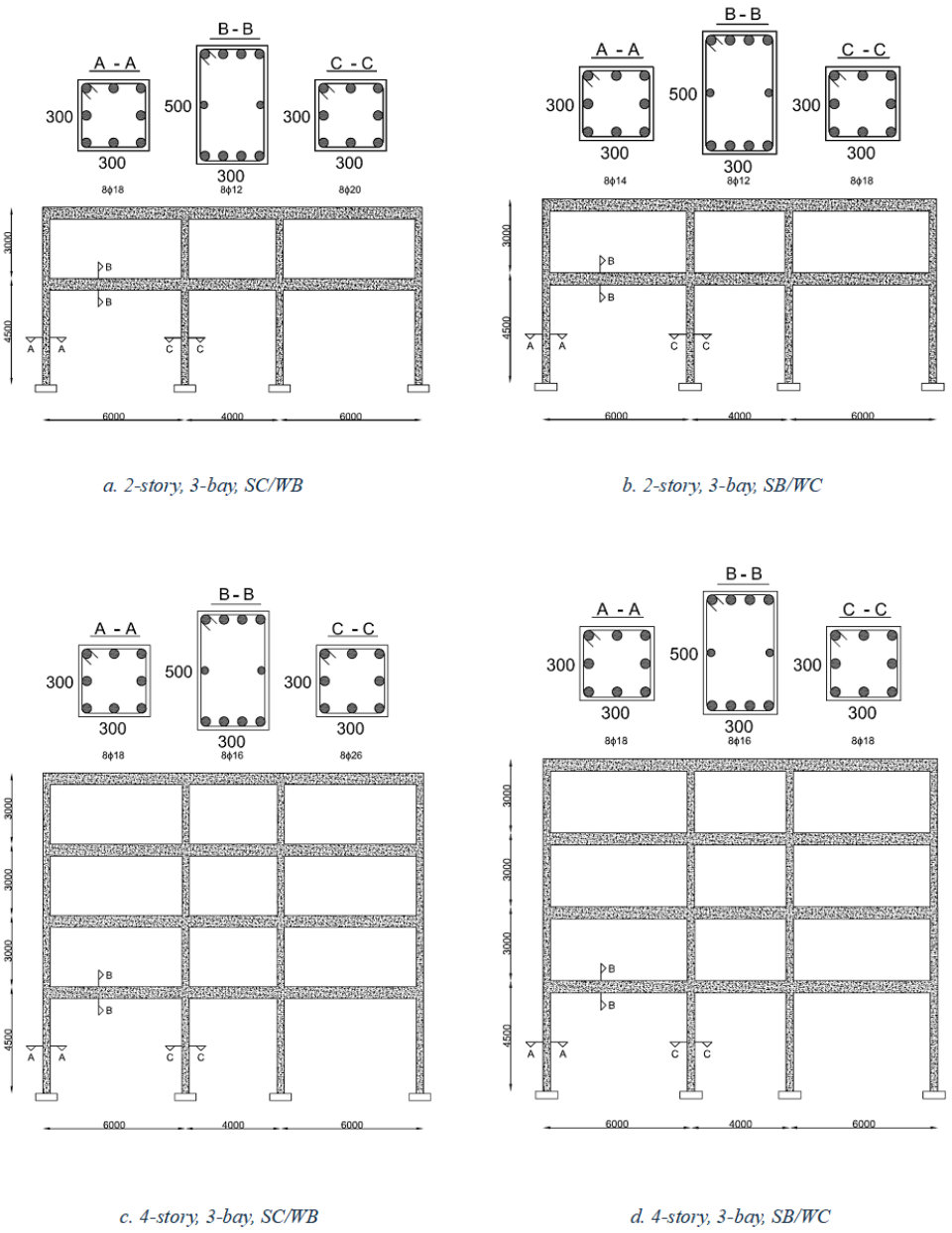

a. 2-story, 3-bay, SC/WB

b. 2-story, 3-bay, SB/WC

c. 4-story, 3-bay, SC/WB

d. 4-story, 3-bay, SB/WC

Figure 1: 2D elevation view of the 2-story, 4-story frames and Cross-section details: A visual comparison showing the reinforcement layout for the "Strong Column" vs. "Strong Beam" archetypes

3.2 Modeling approach

The modelling phase addressed both the nonlinear response of the RC frames and, in a simplified manner, the soil–structure interaction effects associated with the activation of post-earthquake settlements.

3.2.1 Modeling of RC-Frames

The numerical modelling strategy adopted for RC-frames is based on a distributed plasticity approach, adopted to accurately capture the nonlinear response of the RC frames under both seismic and settlement loading. Beam and column members are modelled using fibre-discretised cross-sections, in which the nonlinear behaviour arises from the constitutive response of the constituent materials.

Concrete behaviour is simulated using the uniaxial Popovics material model in [15] (Concrete04 available in the OpenSees material library), incorporating degraded linear unloading–reloading stiffness according to the Karsan–Jirsa formulation and a tensile response characterised by exponential softening in [16]. The concrete constitutive law is defined through seven parameters (Table 1): the compressive strength at 28 days f_c, the strain at peak compressive strength ε_c, the ultimate crushing strain ε_{cu}, the initial elastic modulus E_c, the maximum tensile strength f_{ct}, the ultimate tensile strain ε_t, and the parameter β governing the residual tensile stress decay. The adopted values are $f_c = 38.59\,\text{MPa}$, $\varepsilon_c = 0.0022$, $\varepsilon_{cu} = 0.0141$, $E_c = 32{,}989\,\text{MPa}$, $f_{ct} = 2.05\,\text{MPa}$, $\varepsilon_t = 0.00004$, and $\beta = 0.1$.

Table 1: Parameters characterizing the uniaxial material model Concrete04 selected for concrete material

	f_c [MPa]	e_c [-]	e_{cu} [-]	E_c [MPa]	f_{ct} [MPa]	e_t [-]	b
Beam-column concrete	-38.59	-0.0022	-0.0141	32989	2.05	0.00004	0.1
f_c: compressive strength e_c: strain at the maximum strength e_{cu}: strain at crashing strength E_c: initial stiffness f_{ct}: maximum tensile strength e_{ct}: ultimate tensile strain b: parameter defining residual stress							

Steel reinforcement is modelled using the Giuffré–Menegotto–Pinto uniaxial constitutive law (Steel02 in OpenSees), including isotropic strain hardening. The model is defined by six parameters (Table 2): yield strength $f_y = 521\text{MPa}$, initial elastic modulus $E_0 = 210{,}000\text{MPa}$, strain-hardening ratio $b = 0.03$, and transition parameters $R_0 = 18$, $cR_1 = 0.925$, and $cR_2 = 0.15$, which control the smoothness of the transition from elastic to plastic behaviour.

Perfect bond between steel reinforcement and surrounding concrete is assumed, and bond–slip effects are therefore neglected. The parameters adopted for both constitutive models are summarised in Table 1 and Table 2 and were derived from material characterisation tests reported in previous experimental studies in [11, 17], complemented by values recommended in national design codes. Additional details on the modelling assumptions and calibration procedures can be found in [18], where a similar numerical framework was employed.

Both beams and columns are modelled using force-based beam–column elements (OpenSees *forceBeamColumn* formulation) with Gauss–Lobatto integration. Each structural member is

subdivided into two elements, each characterised by three integration points, in order to ensure an adequate representation of curvature distribution and plastic hinge development along the member length.

Table 2: Parameters characterizing the uniaxial material model Steel02 selected for steel material of bars composing the steel reinforcement of columns and beams

	f_y [MPa]	E_0 [MPa]	b [-]	R_0	c_{R1}	c_{R2}
beam – columns bars	521	210000	0.03	18	0.925	0.15
f_y: yield strength E_0: initial elastic tangent b: strain hardening R_0; c_{R1}; c_{R2}: parameters controlling the transition from elastic to plastic branches (here set equal to the average of recommended values)						

3.3 Modelling of soil-structure interaction

With regard to the soil–structure interaction modelling, a simplified and intentionally decoupled approach is adopted, coherently with the objectives of the present study and with the structural-focused nature of the proposed analysis. The adopted modelling strategy is conceived to represent the structural consequences of post-earthquake settlements, rather than to simulate the geotechnical mechanisms governing soil response and settlement development.

The settlement analysis is therefore carried out by imposing controlled vertical displacements through a simplified soil–structure interface model, under the assumption that the ground deformation has already occurred and must be transferred to the superstructure for post-earthquake structural assessment purposes.

To this aim, settlement is imposed through a set of dedicated “soil nodes”, connected to the column base nodes by means of nonlinear zero-length spring elements. As schematically shown in Figure 2, the two nodes defining each spring element share the same spatial coordinates as the corresponding column base. One node represents the structural base of the column, while the other represents the settled ground. The ground node is fixed in translation and rotation, whereas the column base node is restrained against horizontal translation and rotation but free to move vertically, thus allowing vertical displacements during the settlement phase.

Rather than applying vertical displacement directly to the column bases, a model was adopted in which it is transferred to the structure via defined interface elements. In this context, compatibility between the vertical displacements of the column base and soil nodes was achieved by linking them using the equalDOF command in Opensees.

Zero-length interface elements are defined with unidirectional behaviour and only transmit forces under compression or tension. In this study, springs were assigned a sufficiently large stiffness for compression only to keep deformations negligible compared to the applied settlement. This ensured effective load transfer with nearly zero displacement due to interface deformation when the column pressed into the ground. Under tension, the situation is achieved by used elastic-perfectly plastic uniaxial material that exhibits zero or near-zero stiffness under tensile force and prevents the formation of artificial stress reactions, thereby ensuring that the springs are deactivated in a manner that simulates uplift or loss of contact between the soil and the structure.

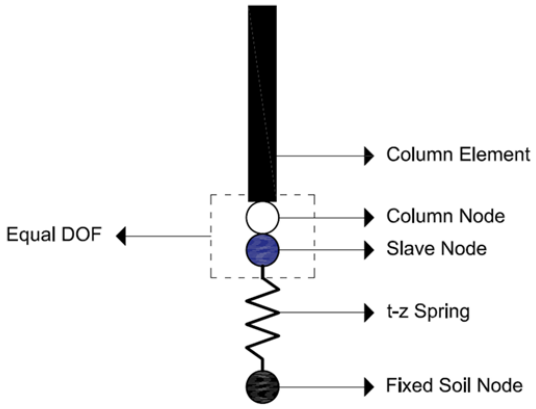

Figure 2: Soil-structure interface modeling strategy

The settlement is defined by the controlled procedure of incrementally applying the vertical displacement dictated by the time series to ground nodes with single-point constraints. This enables the frame to adapt gradually to the applied ground deformation, rather than disturbing it directly, thereby allowing the load redistribution mechanism and contact loss to activate naturally.

When the ground node starts to move vertically, the frame has no choice but to conform to the imposed geometry. The reason behind this is frame's gravity loads, stiffness and load redistribution mechanism. Columns experiencing larger settlements progressively shed axial load, which is redistributed through beam action to adjacent supports. In some settlement profiles that can be categorized as irregular, or in the case of block settlement profiles, a mechanism that traditional settlement analyses cannot observe may arise. Depending on the settlement profile, some columns may lose their connection to the ground, causing a loss of support reaction. In this case, the column behaves as a column suspended by the frame. In the adapted model, in such a situation, the interface spring is disabled, thus the support reaction drops to zero, and the phenomena of uplifting and gap formation are simulated consistently without introducing false constraints.

Compared to traditional modelling strategies in which settlements are directly imposed at column bases and often assumed uniform or idealised, the proposed approach allows capturing essential kinematic features such as settlement gradients, angular distortion, and partial loss of support. At the same time, it deliberately avoids the complexity of fully coupled soil–structure interaction models. The approach should therefore be interpreted as a simplified, structurally oriented framework aimed at investigating the redistribution of forces and damage within the superstructure under a prescribed settlement demand, rather than as a predictive model of soil behaviour.

4 Numerical analyses

The numerical investigation is structured into consecutive and logically connected phases, aimed at reproducing the multi-stage loading history considered in the study and at clearly isolating the effects of seismic damage on the subsequent settlement response. First, nonlinear dynamic analyses are performed to characterise the seismic response of the RC frames and to define the residual damage state induced by ground shaking. Second, nonlinear static analyses are carried

out to evaluate the structural response to imposed foundation settlements, both for undamaged and damaged configurations. A two-step uncoupled sequential analysis framework is adopted to consistently combine seismic and settlement actions, allowing a direct comparison between settlement-only and earthquake–settlement scenarios.

This organisation ensures that the numerical results presented in the following sections can be interpreted in a coherent manner, with each analysis phase providing the necessary mechanical state and reference metrics for the subsequent one.

4.1 Seismic analysis

The seismic response of the RC frames was investigated through nonlinear dynamic time-history analyses. A set of seven spectrum-compatible accelerograms was selected from the European Strong-motion Database (ESD) using the REXEL software, in accordance with the elastic target spectrum for the site of Mirandola, Italy (LON: 11.1, LAT: 44.9). The target spectrum is characterised by a peak ground acceleration $a_g = 2.08\text{m/s}^2$, a soil factor $F_0 = 2.50$, and a corner period $T_C^* = 0.27\text{s}$, consistent with Eurocode 8 Site Class C conditions. A return period of $T_R = 2475\text{years}$ was, in order to subject the frames to severe seismic excitation. Details of the selected records and their spectral compatibility are reported in Table 3 and Figure 3.

Table 3: Details of the account sets of accelerograms spectrum compatible

Earthq. ID	Station ID	Earthquake Name	Date	Mw	Fault Mech.	Epic. Dist. [km]	PGA [m/s^2]
81	ST46	Basso Tirreno	15/04/1978	6	oblique	18	0.7188
286	ST223	Umbria Marche	26/09/1997	6	normal	22	1.0406
561	ST549	Adana	27/06/1998	6.3	strike slip	30	2.6442
474	ST1253	Ano Liosia	07/09/1999	6	normal	19	0.9941
65	ST33	Friuli (aftershock)	15/09/1976	6	thrust	11	0.8838
158	ST121	Alkion	25/02/1981	6.3	normal	25	1.176
157	ST121	Alkion	24/02/1981	6.6	normal	20	2.2566

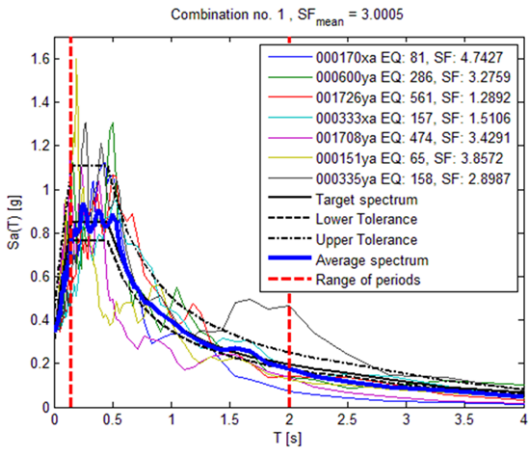

Figure 3: Spectra of the accounted accelerogram (thin lines); average spectrum of selected accelerogram (thick line); target spectrum from the code

Each analysis began with the application of gravity loads, which were kept constant throughout the subsequent dynamic phase. After static equilibrium was achieved, nonlinear time-history analyses were carried out using the selected ground motions. At the end of each accelerogram, a rest phase was introduced by appending a 60-second interval of zero acceleration.

This procedure allowed the structure to dissipate kinetic energy and reach a stable residual configuration, ensuring that permanent deformations could be evaluated without interference from transient free vibrations.

The damage state induced by seismic loading was quantified in order to define the initial conditions for the subsequent settlement analyses. Three complementary indicators were adopted. Global stiffness degradation was assessed through the elongation of the fundamental period, obtained by comparing the initial and post-earthquake values. Permanent geometric nonlinearity was quantified through residual inter-storey drift ratios, which represent the persistence of asymmetric configurations and non-zero internal forces after shaking.

At the local level, damage was evaluated by monitoring curvature demand at critical sections; maximum and residual curvatures were compared with yield and ultimate limits to quantify the consumption of ductility and the remaining rotational capacity available to accommodate subsequent settlement-induced deformations.

4.2 Settlement analysis

The response of the frames to foundation settlements was analysed through nonlinear static incremental analyses. In a first step, vertically distributed gravity loads were applied to the beams and the equilibrium configuration under permanent loads was established. Starting from this condition, settlement was imposed by introducing two distinct settlement patterns, each characterised by two different configurations at the foundation level, in order to simulate the quasi-static evolution of ground deformations associated with post-liquefaction reconsolidation.

Settlement demand was applied using a displacement-controlled protocol. Vertical displacements were incrementally imposed at the soil nodes, corresponding to the fixed nodes of the zero-length interface elements, rather than being directly prescribed at the column bases. This modelling strategy allows the soil–structure interface to govern load transfer naturally. When the imposed downward displacement exceeds the tendency of the structure to follow the settlement, due to frame stiffness or arching mechanisms, the compression-only springs deactivate, reproducing loss of contact and hanging-column behaviour.

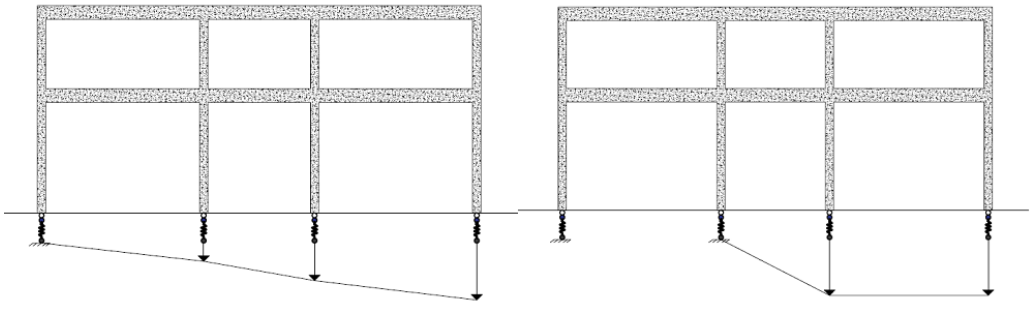

a. Settlement pattern 1 Sloped line (0, 40, 130, 200 mm). b. Settlement pattern 2 Block drop (0, 0, 400, 400 mm).

Figure 4: Settlement Patterns / Schematic diagrams of the frame foundation line

The analyses were carried out incrementally until the target settlement values were reached, equal to 200 mm for Pattern 1 and 400 mm for Pattern 2 (Figure 4), or until numerical instability occurred. During the analyses, the residual settlement capacity of the frame was defined through

a local damage criterion, namely the vertical displacement at which the first structural section reached its ultimate curvature limit ϕ_u. This limit state represents a conservative threshold associated with serviceability and repairability at the section level and is clearly distinct from global instability, which typically occurs at much larger settlement values due to the redundancy of the frame system.

4.3 Seismic and settlement Sequential loading strategy

As illustrated in Figure 5, a sequential analysis has been developed to simulate real-life multi-hazard scenarios which is the motivation for this research. As outlined in Sections 5.1 and 5.2, the analyses begin with the application of gravitational forces, followed by earthquake and settlement analyses, which are then combined to evaluate the cumulative impact of seismic damage and subsequent settlement.

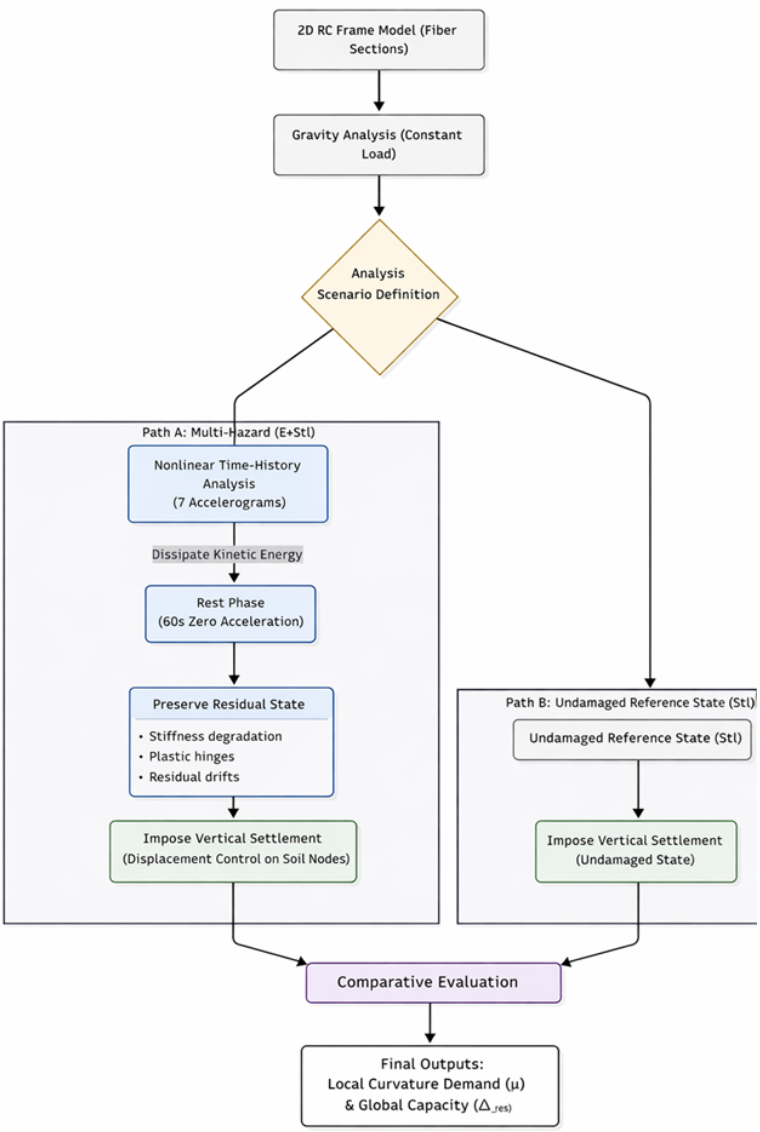

Figure 5: Flowchart of the adopted sequential numerical procedure, illustrating the comparison between settlement-only analyses and earthquake–settlement analyses performed on pre-damaged frames, and the resulting assessment of local and global performance indicators

The two-stage uncoupled sequential analysis starts with nonlinear dynamic excitation. After earthquake loading, the frame is put into a resting state as detailed in Section 5.1, preserving the hysteresis experienced during the earthquake. The resulting mechanical state (stiffness degradation, residual inter-story drift, accumulated plastic strain, and internal force redistribution) is then transferred to the next stage as the initial condition.

In the final stage, the prescribed settlement is applied to the pre-damaged structure under the initial conditions described above via soil nodes. Thus, the effect of seismic damage on the structure during subsequent settlement is simulated chronologically. Results obtained from the sequential analysis, achieved by consistently linking dynamic and static analyses, are compared with those from settlement-only analysis (applied to an undamaged structure). The comparative nature of this study helps to clearly define and quantify the earthquake-induced structural changes that occur. It helps to understand how pre-existing damage affects global and local damage mechanisms and changes in settlement capacity.

5 Results overview and comparison framework

The results are presented by consistently distinguishing three analysis scenarios, which are used throughout the following sections:

(i) Earthquake-only (E): nonlinear time-history analyses on fixed-base frames, providing the residual damaged state at the end of shaking.

(ii) Settlement-only (Stl): nonlinear static incremental settlement analyses applied to the undamaged RC-frame.

(iii) Sequential earthquake + settlement (E+Stl): settlement analyses applied to the post-earthquake residual state obtained from scenario E, preserving stiffness degradation, residual inter-storey drifts, accumulated plastic strains, and the internal force distribution.

This organisation is adopted to avoid ambiguities in the interpretation of “damaged” versus “undamaged” settlement response. In particular, global settlement mechanisms and force redistribution are discussed by comparing Stl and E+Stl cases for the same settlement pattern, while local damage and residual settlement capacity are evaluated by tracking curvature demand and the attainment of ultimate curvature limits under the two scenarios.

5.1 Seismic damage assessment (scenario E)

The seismic damage of the SC/WB and SB/WC RC frames obtained from nonlinear time-history analyses was first quantified through global response indicators, in order to characterise the overall degradation of the structural systems prior to the application of foundation settlements. Fundamental period elongation and inter-storey drift demands were adopted as primary global indicators and are reported in Table 4 and Figure 6, respectively.

Table 4 shows that, after the seismic analyses, both frame typologies exhibited a significant increase in the fundamental period due to residual damage. For the 2-storey frames, the initial period was approximately 0.43–0.44 s (undamaged), while post-earthquake values ranged approximately between 0.64 s and 0.90 s depending on the record and detailing. For the 4-storey frames, the initial period was approximately 0.67–0.70 s (undamaged), while post-earthquake values ranged approximately between 0.86 s and 1.30 s. This elongation corresponds to an estimated stiffness reduction of about 55%–73% (depending on the selected ground motion), reflecting widespread cracking and yielding developed during the earthquake response. Despite record-to-record variability, the post-earthquake periods show limited scatter, suggesting

that the frames reached a residual damaged configuration characterised by a comparable global stiffness level.

Table 4: Fundamental Period (T_1): Initial vs. Post-Earthquake for all 7 records

	2 story		4 story	
	SC/WB T1(s)	SB/WC T1(s)	SC/WB T1(s)	SB/WC T1(s)
Undamaged	0.43	0.44	0.6691	0.6981
Eq. ID-81	0.7044	0.7370	1.0681	1.1466
Eq. ID-286	0.7526	0.8400	1.1312	1.2439
Eq. ID-561	0.8178	0.8995	0.8562	1.262
Eq. ID-474	0.6417	0.6944	0.9706	0.9736
Eq. ID-65	0.7690	0.9048	1.0516	1.0816
Eq. ID-158	0.7272	0.8112	1.0630	1.3027
Eq. ID-157	0.8288	0.8866	1.0740	1.2046

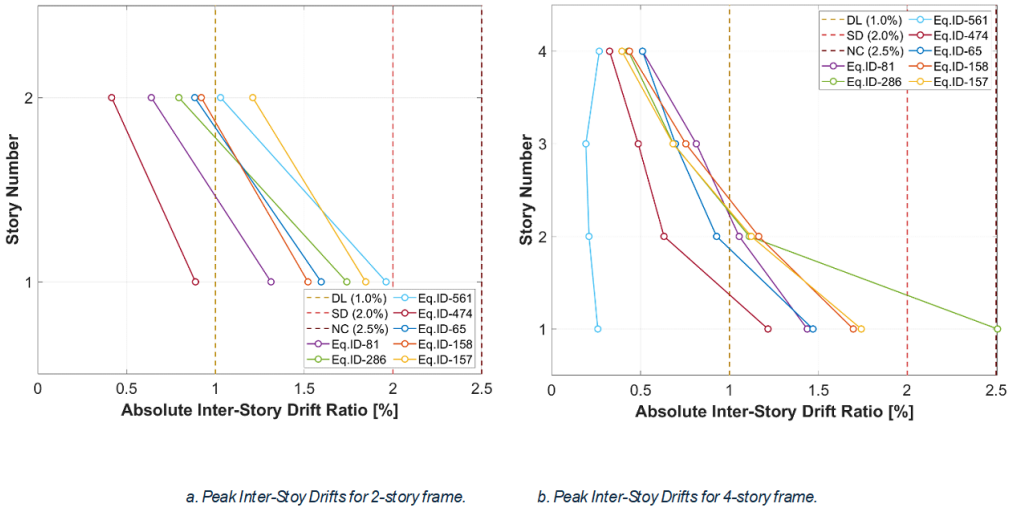

Figure 6: Scatter plot of Max Inter-story Drift for the 7 records, with Eurocode limit lines (DL, SD, NC) drawn horizontally

The maximum values of inter-storey drift ratios were also examined and compared with the Eurocode 8 performance limits. As shown in Figure 6, the peak drift demands generally exceeded the Damage Limitation threshold and, in several cases, approached or exceeded the Significant Damage limit state.

Although the two frames were designed according to different detailing philosophies, their global damage indicators after seismic loading were broadly comparable. Both SC/WB and SB/WC configurations experienced similar levels of period elongation and global stiffness degradation, indicating that the overall severity of seismic-induced global degradation is comparable.

However, differences clearly emerge in the distribution of damage within structural members. In the SC/WB frames, damage is mainly concentrated in beams, where plastic hinges develop as intended by capacity design principles. Columns remain largely elastic or experience limited nonlinear demand, preserving their axial load-carrying capacity. Conversely, in the SB/WC frames, columns are more directly involved in the nonlinear response, with higher

curvature demands at column ends, while beams exhibit a more limited damage level. Therefore, detailing philosophy primarily influences the location of damage rather than the overall reduction in global stiffness, with potentially relevant implications for the local response during the subsequent settlement phase.

5.2 Settlement and sequential effects (scenarios Stl and E+Stl)

5.2.1 Global response

The settlement response of the RC frames was investigated by imposing vertical displacements at the foundation level and evaluating the structural response under both Stl and E+Stl scenarios. The objective of this section is to identify the governing global mechanisms activated during settlement and to assess whether, and to what extent, these mechanisms are affected by the presence of pre-existing seismic damage.

Across all analysed configurations, settlement consistently activated global load-transfer mechanisms. As support conditions progressively evolved, internal forces were redistributed to maintain equilibrium, and alternative load paths developed through the continuity of beams and adjacent columns. Within the analysed settlement range, global stability was preserved even under large imposed settlements, for both settlement patterns and both design configurations (SC/WB and SB/WC).

A key outcome of the comparison between Stl and E+Stl scenarios is that the global kinematic mechanisms remain essentially unchanged. The overall deformation shape, the sequence of force redistribution, and the evolution of support reactions follow the same trends in both cases. This indicates that, at the global equilibrium level, settlement response is primarily governed by frame geometry and by the imposed settlement profile, whereas the seismic history mainly influences the initial residual state rather than the subsequent redistribution mechanism.

This behaviour is also reflected in the axial-force redistribution observed during settlement. Settlement produced a pronounced reallocation of axial forces among columns, characterised by load shedding at settling supports and force increases in adjacent columns. Figure 7 provides a representative example for the 2-storey, 3-bay SC/WB frame under settlement Pattern 1, showing the evolution of normalised axial force versus imposed settlement. In the figure, black lines refer to Stl analyses, while red lines refer to E+Stl sequential analyses (one curve for each seismic record).

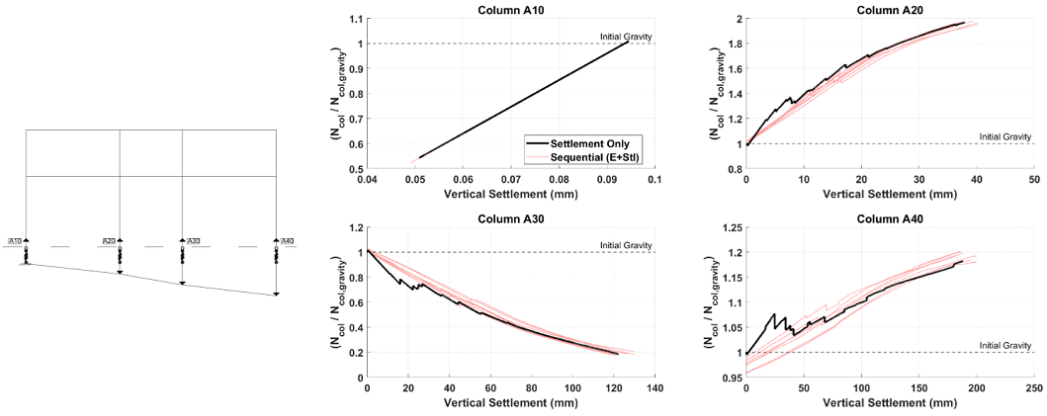

Figure 7: Scheme of frame and settlement profile (left); Normalized axial force vs. vertical settlement of column sections at the base of two-story SC/WB frame

In several cases, neighbouring columns attract axial forces approaching twice the original gravity load (e.g., Figure 7, secA20), highlighting the activation of arching effects and alternative load-transfer paths. Importantly, the force–settlement curves show nearly parallel trends for Stl and E+Stl cases: while the initial axial-force levels may differ due to residual seismic effects, the slopes are very similar. This confirms that the axial-force redistribution mechanism during settlement is largely independent of the prior seismic damage state, and remains mainly controlled by geometry, continuity of load paths, and the imposed settlement configuration.

For settlement configurations characterised by high displacement gradients (Pattern 2), an additional global mechanism was observed, namely the activation of a hanging-column behaviour (Figure 8). When the imposed settlement at a column base becomes sufficiently large, compression-only supports allow progressive loss of contact between the column and the supporting soil. As uplift conditions develop, the settling column is no longer forced to follow the downward displacement imposed at the soil node: partial detachment occurs and the column behaves as a hanging element supported by the surrounding frame. As a consequence, the effective vertical displacement transmitted to the superstructure becomes lower than the displacement imposed at the soil level, resulting in a partial soil–structure decoupling at large settlements (Figure 8).

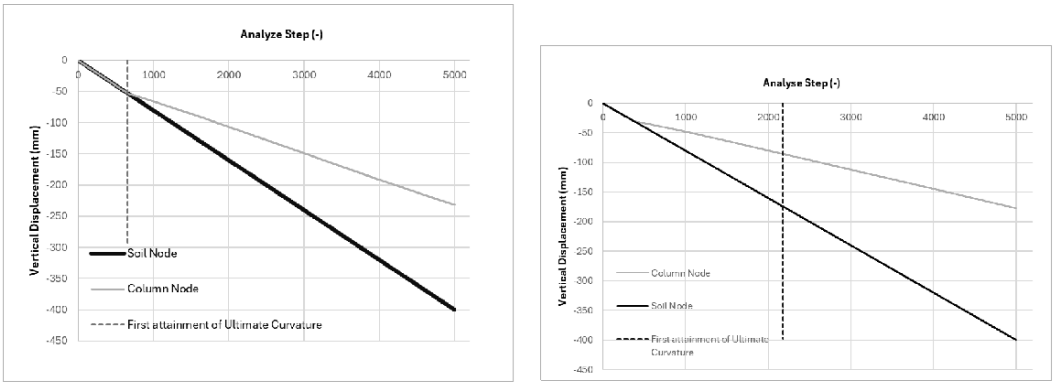

a. 2-story SC/WB frame *b. 4-story SC/WB frame*

Figure 8: The hanging column mechanism

The activation of this mechanism contributes to preserving global equilibrium. Even for very large imposed settlements, the frame maintains stability through the combined action of force redistribution and partial support loss. Within the analysed settlement range, no global collapse was observed; however, local damage may still accumulate and govern structural performance in terms of repairability and local limit states.

5.2.2 Local damage mechanisms

Local damage during both the seismic and settlement phases was evaluated in terms of curvature ductility demand at critical sections. For each monitored section, two reference limits were identified: the yielding limit, corresponding to the onset of nonlinear behaviour, and the ultimate curvature limit, associated with severe damage and loss of deformation capacity. These limits were used to track the evolution of local damage throughout the sequential loading process and to define the residual settlement capacity discussed in the previous section.

The adoption of curvature ductility as a local damage metric is particularly suitable for the investigation conducted in this paper, as settlement-induced effects primarily manifest through

compatibility-driven bending demands rather than through global instability mechanisms. Curvature demand therefore provides a direct measure of how local deformation capacity is consumed under combined seismic and settlement actions.

A key outcome of the local response analyses is the identification of a clear state change induced by seismic loading, which significantly alters the subsequent response to foundation settlements. Several structural sections that remained elastic when settlements were applied to the undamaged structure (Stl scenario) developed plastic behaviour when the same settlement profiles were imposed after the seismic phase (E+Stl scenario). This behaviour is consistently observed across the analysed configurations and settlement patterns.

The reason for the aforementioned mechanism is residual curvature, one of the permanent damages caused by earthquakes on structures. Although the structure maintains its global equilibrium after seismic loading, permanent deformations in critical sections cause non-zero curvature demands. Subsequent settlement also causes curvature demands in critical sections, depending on the geometric configuration. In this case, if settlement causes curvature demands on sections already damaged by the earthquake, the relevant sections reach their ultimate and yield curvature limits earlier. To illustrate this clearly, Figure 9 shows the approximate section's locations and Figure 10 compares the curvature demands created by the Stl vs E + Stl scenarios in some critical sections.

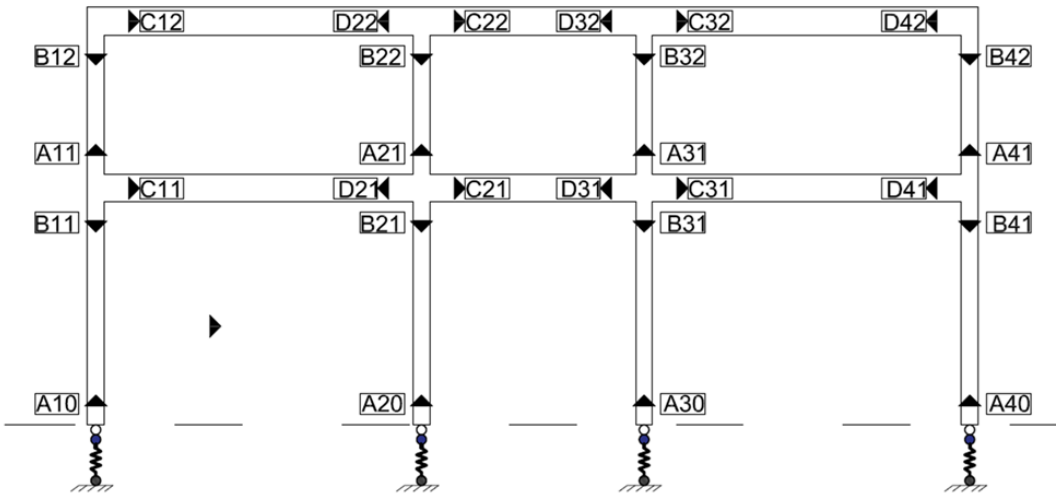

Figure 9: Scheme of the 2-story frame with labels of monitored sections

As confirmed by the results obtained, earthquake-induced damage may not alter the settlement-induced global redistribution mechanism or the overall equilibrium path. However, it has been observed that it changes the internal mechanical state, increases the amount of local deformation during settlement, and reduces ductility. This finding demonstrates that post-earthquake settlement capacity cannot be reliably assessed without explicitly accounting for residual seismic damage, even when global damage indicators suggest comparable levels of stiffness degradation.

Comparing the SC/WB and SB/WC frames indicates that the same structural regions generally govern the local response during settlements for both design philosophies: column bases and beam–column joints adjacent to the settling supports. However, significant differences emerge in the distribution of residual curvature after seismic loading. In SC/WB frames, residual curvature is predominantly concentrated in the beams, whereas the columns retain a larger portion of their deformation capacity. This damage pattern enables settlement-induced demands

to be accommodated without immediately endangering the safety of the columns. Conversely, in SB/WC frames, residual curvature demands are more pronounced in columns, resulting in reduced available ductility during settlement. Figure 11, demonstrates Ductility Demand vs. Load Case of beam section sec.D41: a. two-story SC/WB frame; b. two-story SB/WC frame for the same loading conditions (E + Stl with Settlement Pattern 1).

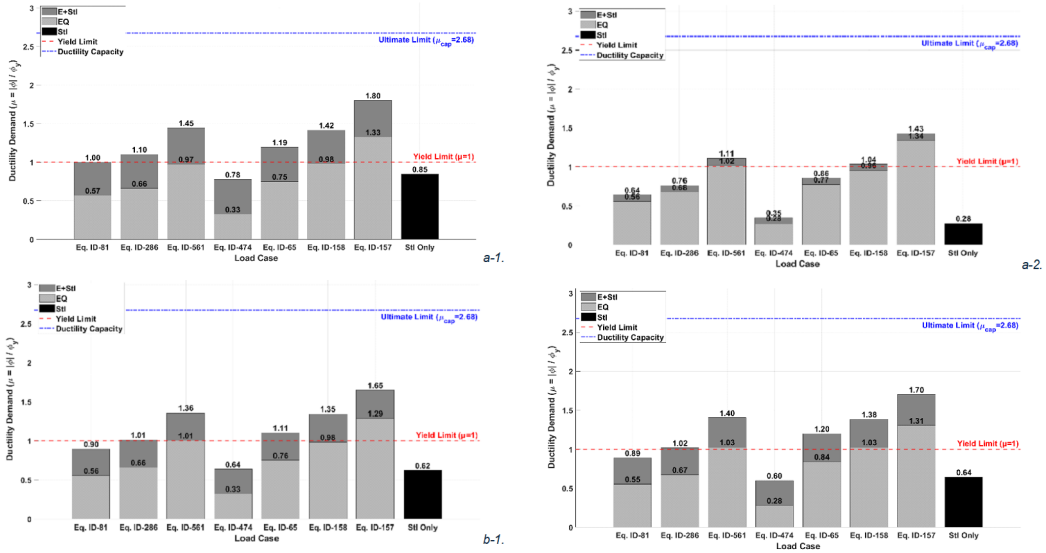

Figure 10: Ductility Demand vs. Load Case of 2-story SC/WB frame: a-1. beam section of sec.D21 for settlement pattern 1; a-2. beam section of sec.D41 for settlement pattern 1; b-1. beam section of sec.D21 for settlement pattern 2; b-2. beam section of sec.D21 for settlement pattern 2

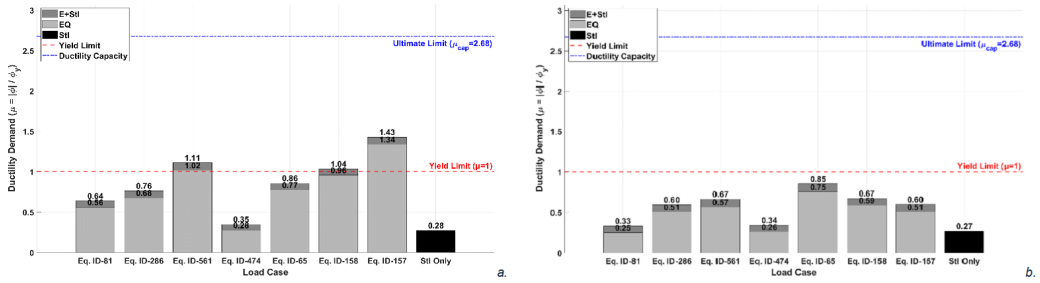

Figure 11: Ductility Demand vs. Load Case of beam section sec.D41: a. two-story SC/WB frame; b. two-story SB/WC frame

Consequently, older design configurations may exhibit delayed beam damage activation during settlement, but this occurs at the expense of increased column involvement during seismic loading and reduced column ductility. This trade-off does not imply improved performance of non-ductile systems; rather, it demonstrates how different design approaches control the location of residual damage and, consequently, the sections that determine post-earthquake settlement vulnerability.

Overall, the local damage analyses explain the apparent decoupling observed between global stability and structural performance under post-earthquake settlements. While global equilibrium is preserved through force redistribution mechanisms, local curvature-controlled limit

states govern the residual settlement capacity and define the onset of damage relevant to repairability and post-earthquake decision-making.

6 Discussion

The results highlight a clear decoupling between global equilibrium and local failure mechanisms during post-earthquake foundation settlements. For all examined configurations, the RC frames maintained overall stability for settlement levels substantially larger than those associated with the attainment of local curvature limits at critical sections. This confirms that, within the considered range of imposed ground deformations, the structural response to settlement is primarily accommodated through global force redistribution and alternative load paths, while structural performance is ultimately governed by local ductility consumption.

Accordingly, foundation settlements should be interpreted mainly as a local ductility and repairability hazard, rather than a direct trigger of global collapse for the investigated frame typologies. Although the structural system remains globally stable due to redundancy and redistribution mechanisms, severe local damage may develop in columns and beam–column joint regions, potentially compromising repairability, safety margins, and post-event functionality. Therefore, global stability alone is not a sufficient indicator of structural performance under post-earthquake settlement conditions.

A key implication is that settlement assessments performed on undamaged structural models can be unconservative. The analyses show that sections remaining elastic under settlement-only conditions may yield or reach ultimate curvature limits when the same settlement profiles are applied after seismic loading (Figure 12 shows the comparison of plastic hinge status for settlement-only and sequential cases). This behaviour is driven by the residual seismic state: permanent curvatures and plastic strains accumulated during the earthquake phase pre-consume part of the available ductility and amplify settlement-induced curvature demand. Consequently, post-earthquake assessment procedures should explicitly account for the damaged residual configuration, rather than relying on idealised undamaged models, even when global response indicators suggest acceptable behaviour.

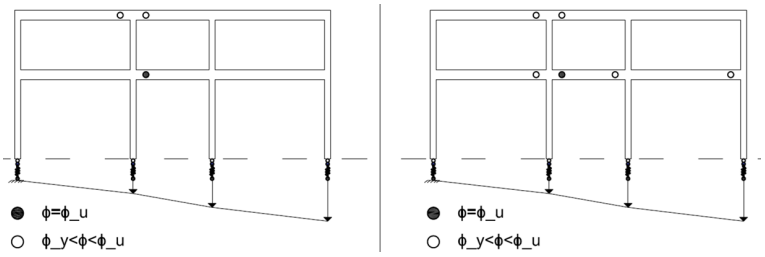

Figure 12: Plastic Hinge Distribution Map of 2-story SC/WB frame for Settlement Pattern 1 with colored dots. Left Frame: Settlement Only (Localized damage). Right Frame: Sequential Case (Distributed damage + same failure point)

The results discussed above refer to a specific seismic action level, defined through spectrum-compatible ground motions characterised by a target PGA corresponding to the selected site conditions. A natural question arising from this choice is whether the observed decoupling between global settlement mechanisms and local damage evolution is inherently linked to this specific seismic intensity, or whether it remains valid when the severity of ground shaking is varied.

In order to address this issue and evaluate the validity of the proposed interpretations, a sensitivity study must be conducted by scaling the seismic input intensity. It is also necessary to determine the critical range within which seismic intensity can be increased. This range is defined as the point at which the structure sustains severe damage at its ultimate limit state (ULS), yet remains stable enough to withstand subsequent ground settlement. The seismic scaling factor coefficients that satisfy this condition for the relevant frames have been found to be in the range 1.0–1.2. For instance, a scaling factor of 1.3 caused an attainment of the ultimate curvature for Record 6 (Eq. ID-158) during seismic activity.

Within this intensity range, the main conclusions of the study remain unchanged. At the global level, the evolution of axial-force redistribution during settlement was essentially the same for the reference and increased seismic intensities, as shown in Figure 13 and Figure 14. Once the earthquake had driven the structure into a damaged residual state, further increases in seismic intensity did not alter the subsequent settlement-induced redistribution mechanisms. This indicates that global load redistribution during settlement is primarily controlled by frame geometry and by the imposed settlement profile, rather than by incremental differences in the severity of seismic damage.

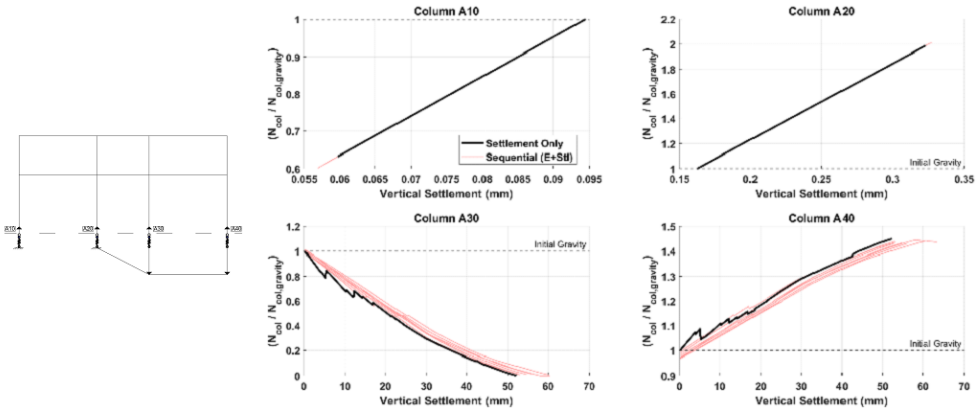

Figure 13: Scheme of frame and settlement profile (left); Normalized axial force vs. vertical settlement of column sections at the base of two-story SC/WB frame - S.F. = 1.0 .

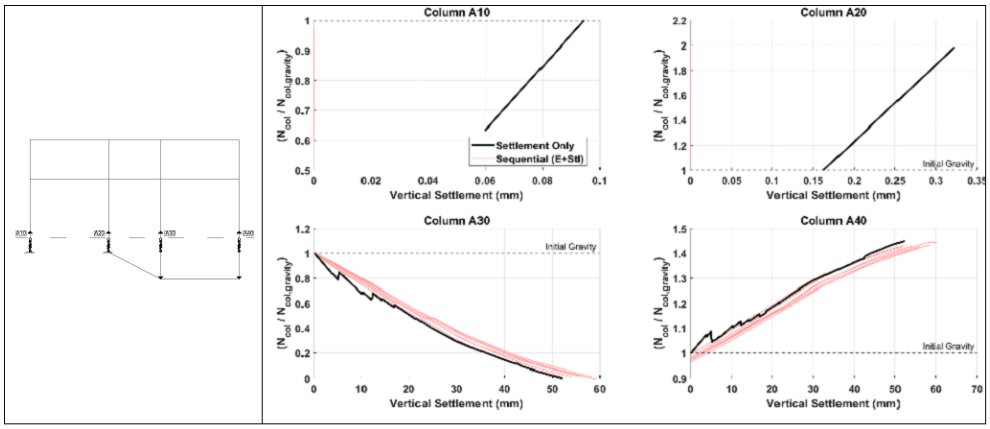

Figure 14: Scheme of frame and settlement profile (left); Normalized axial force vs. vertical settlement of column sections at the base of two-story SC/WB frame - S.F. = 1.2

At the local level, higher seismic intensity led to a modest increase in residual curvatures; however, the governing failure mechanisms and the critical sections remained consistent, as illustrated in Figure 15. This behaviour supports the interpretation of a threshold-type "state change" triggered by yielding, after which settlement vulnerability is primarily controlled by geometric distortion rather than by the exact magnitude of seismic demand, provided global stability is preserved.

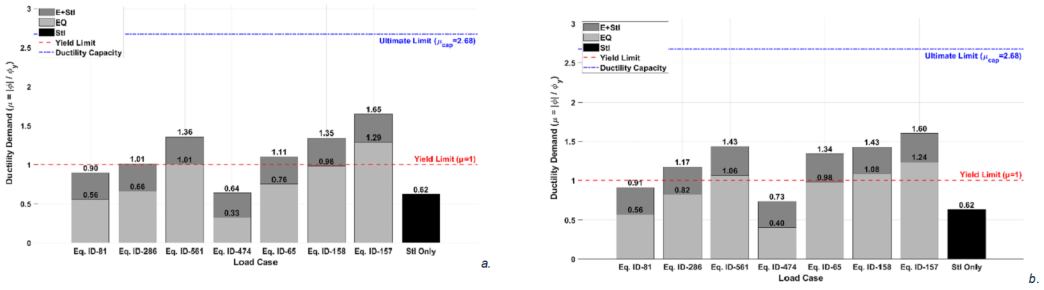

Figure 15: Ductility Demand vs. Load Case of beam section sec.D21 - two-story SC/WB frame: a. S.F. 1.0; b. S.F. 1.2

In light of the findings, it would be beneficial to consider post-earthquake assessment strategies at two levels. At the global level, assessing stability conditions and redistribution mechanisms according to structural geometry and settlement configurations can be effective. However, section-based investigations at the local level are also important. Parameters such as curvature demand, residual ductility and damage accumulation have been shown to be significantly affected in the examined context, implying that the local limit state may be reached before global equilibrium is lost.

Finally, it is noted that the adopted framework is intentionally structural-focused and relies on prescribed settlement profiles imposed after the seismic phase. As such, the results are most directly applicable to scenarios where the dominant settlement component develops after strong shaking (e.g., post-liquefaction reconsolidation), while fully coupled soil–structure interaction effects during shaking are not captured. Within this intended scope, the proposed sequential strategy provides a practical and physically consistent basis to integrate seismic damage and post-earthquake settlements in engineering decision-making, enabling rapid screening combined with detailed local verification when needed.

7 Conclusions

This study examined the influence of seismic-induced damage on the subsequent response of reinforced concrete moment-resisting frames subjected to post-earthquake foundation settlements by means of a decoupled sequential analysis framework. The adopted approach allowed seismic and settlement effects to be consistently combined while preserving the residual mechanical state reached at the end of the earthquake. Both modern Strong Column/Weak Beam and older Strong Beam/Weak Column configurations were considered to investigate the role of structural detailing on post-earthquake settlement vulnerability.

The results show that the global mechanisms activated during settlement, including axial force redistribution, arching action, and partial loss of support contact, are governed primarily by structural geometry and by the imposed settlement profile, and are only marginally influenced by prior seismic damage. As a consequence, the global capacity of the frames to main-

tain equilibrium under large imposed settlements remains largely unchanged when comparing settlement-only and sequential earthquake–settlement scenarios.

In contrast, seismic loading induces a marked state change at the local level. Residual plastic deformations and permanent inter-storey drifts accumulated during the earthquake phase partially exhaust the available ductility of critical sections, modifying the internal stress and deformation state from which settlement demand subsequently develops. This leads to a clear decoupling between global stability and local failure: while global equilibrium is preserved for settlement levels well beyond those associated with local curvature limits, critical sections may reach yielding or ultimate curvature at relatively low settlement values. This behaviour, synthetically illustrated by the comparison between Settlement-Only and Sequential cases in Figure 12, confirms that post-earthquake settlements primarily represent a local ductility and repairability hazard rather than a global collapse hazard, and that global stability alone is not a sufficient indicator of structural performance under combined seismic and settlement actions.

The comparison between Strong Column/Weak Beam and Strong Beam/Weak Column configurations further indicates that, although reinforcement detailing strongly affects the distribution of seismic damage, overall settlement vulnerability is mainly controlled by geometric characteristics such as span length and stiffness distribution. Both typologies exhibit comparable global settlement resistance; however, differences in the location of residual curvature after seismic loading lead to distinct local failure patterns. In particular, modern SC/WB frames tend to enter the settlement phase with residual damage concentrated in beams, whereas older SB/WC frames exhibit higher residual curvature demands in columns, resulting in reduced available ductility and earlier attainment of local limit states.

Finally, the study demonstrates that settlement assessments based on undamaged or elastic structural models may lead to unconservative predictions. Sections remaining elastic under settlement-only conditions frequently develop plastic behaviour or reach failure when the same settlement profiles are applied after seismic loading. These findings highlight the necessity of explicitly accounting for residual seismic damage and deformation history in post-earthquake settlement evaluations and support the adoption of sequential analysis strategies as a reliable and physically consistent framework for assessing the vulnerability of existing reinforced concrete frames.

Declaration of generative AI and AI-assisted technologies in the manuscript preparation process

During the preparation of this work, the author(s) used DeepL Write in order to improve the language quality and correct spelling errors. After using this tool/service, the author(s) reviewed and edited the content as needed and take(s) full responsibility for the content of the published article.

References

[1] Burland, J. B., & Wroth, C. P. (1975). Settlement of buildings and associated damage (No. CP 33/75).

[2] Boscardin, M. D., & Cording, E. J. (1989). Building response to excavation-induced settlement. *Journal of Geotechnical engineering, 115*(1), 1-21.

[3] Skempton, A. W., & MacDonald, D. H. (1956). The allowable settlements of buildings. *Proceedings of the Institution of Civil Engineers, 5*(6), 727-768.

[4] Bird, J. F., Bommer, J. J., Crowley, H., & Pinho, R. (2006). Modelling liquefaction-induced building damage in earthquake loss estimation. *Soil Dynamics and Earthquake Engineering, 26*(1), 15-30.

[5] Stewart, J.P., Crouse, C.B., Hutchinson, T., Lizundia, B., Naeim, F., Ostadan, F. (2012). Soil-Structure Interaction for Building Structures. Natl. Inst. Stand. Technol. NEHRP.

[6] Fotopoulou, S., Karafagka, S., & Pitilakis, K. (2018). Vulnerability assessment of low-code reinforced concrete frame buildings subjected to liquefaction-induced differential displacements. *Soil Dynamics and Earthquake Engineering, 110*, 173-184.

[7] Karafagka, S., Fotopoulou, S., & Pitilakis, D. (2021). Fragility assessment of non-ductile RC frame buildings exposed to combined ground shaking and soil liquefaction considering SSI. *Engineering Structures, 229*, 111629.

[8] Negulescu, C., & Foerster, E. (2010). Parametric studies and quantitative assessment of the vulnerability of a RC frame building exposed to differential settlements. *Natural Hazards and Earth System Sciences, 10*(9), 1781-1792.

[9] Bao, C., Xu, F., Chen, G., Ma, X., Mao, M., & Zhang, S. (2019). Seismic vulnerability analysis of structure subjected to uneven foundation settlement. *Applied Sciences, 9*(17), 3507.

[10] Gomez-Martinez, F., Millen, M. D., Costa, P. A., & Romao, X. (2020). Estimation of the potential relevance of differential settlements in earthquake-induced liquefaction damage assessment. *Engineering Structures, 211*, 110232.

[11] Grande, E., Lirer, S., & Milani, G. (2022, March). Simple approach to evaluate the influence of seismic residual displacements on post-liquefaction settlements of RC-frames. In *Structures* (Vol. 37, pp. 411-425). Elsevier.

[12] Miano, A., Mele, A., Del Gaudio, C., Verderame, G. M., & Prota, A. (2024). Updating of the seismic fragility curves for RC buildings subjected to slow-moving settlements. *Journal of Building Engineering, 86*, 108907.

[13] Cetin, K. O., Soylemez, B., Guzel, H., & Cakir, E. (2025). Soil liquefaction sites following the February 6, 2023, Kahramanmaraş-Türkiye earthquake sequence. *Bulletin of Earthquake Engineering, 23*(3), 921-944.

[14] Standard, B. (2005). Eurocode 8: Design of structures for earthquake resistance. *Part, 1*, 1998-1.

[15] Popovics, S. (1973). A numerical approach to the complete stress-strain curve of concrete. *Cement and concrete research, 3*(5), 583-599.

[16] Karsan, I. D., & Jirsa, J. O. (1969). Behavior of concrete under compressive loadings. *Journal of the Structural Division, 95*(12), 2543-2564.

[17] Grande, E., Imbimbo, M., & Yigitbas, M. (2025). A pushover-based simplified approach for predicting post-earthquake residual displacements in low-rise RC frames. *Bulletin of Earthquake Engineering, 23*(11), 4635-4656.

[18] Bagnoli, M., Grande, E., & Milani, G. (2021). Numerical study of the In-Plane seismic response of RC infilled frames. *Construction Materials, 1*(1), 82-94.